

GNSP: Gradient Null Space Projection for Preserving Cross-Modal Alignment in VLMs Continual Learning

Tiantian Peng¹, Yuyang Liu^{1,*}, Shuo Yang¹, QiuHe Hong¹, YongHong Tian^{1,2,*}

^{*}Corresponding Authors

¹Peking University, Shenzhen Graduate School, ²Peng Cheng Laboratory

Abstract

Contrastive Language–Image Pretraining (CLIP) has demonstrated remarkable zero-shot generalization by aligning visual and textual modalities in a shared embedding space. However, when continuously fine-tuned on diverse tasks, CLIP suffers from catastrophic forgetting and degradation of its embedding alignment, undermining its zero-shot capabilities. In this work, we propose Gradient Null Space Projection (GNSP), an efficient continual learning method that projects task-specific gradients onto the null space of previously learned knowledge. This orthogonal projection mathematically prevents interference with previous tasks without relying on rehearsal or architectural modification. Furthermore, to preserve the inherent generalization property of CLIP, we introduce knowledge distillation and combine it with a modality alignment preservation loss inspired by CLIP pre-training to stabilize the structure of the multimodal embedding space during fine-tuning. On the MTIL benchmark consisting of 11 tasks, our method achieved SOTA performance on both the *Average* and *Last* key metrics. More importantly, experiments show that our method successfully maintains the original modality gap and cross-modal retrieval performance of CLIP, confirming its effectiveness in maintaining a robust visual-language space throughout the continual learning process. Code is available at: <https://github.com/Ppp-Ttt/GNSP>.

1 Introduction

Pretrained Vision-Language Models (VLMs), such as CLIP (Radford et al. 2021) and ALIGN (Jia et al. 2021), have demonstrated remarkable capabilities in learning a shared multi-modal embedding space by aligning visual and language features through large-scale contrastive learning. This shared embedding space enables strong zero-shot generalization and makes VLMs effective for various downstream tasks via fine-tuning.

During continual fine-tuning, these models not only suffer from the classic challenge *catastrophic forgetting* in continual learning (CL) (McCloskey and Cohen 1989; Kirkpatrick et al. 2016; Goodfellow et al. 2013), but also face degradation in their generalization ability. This degradation stems from disruption in the shared embedding space, where the alignment between visual and language modalities begins to drift. When VLMs are fine-tuned on new tasks, the gradient

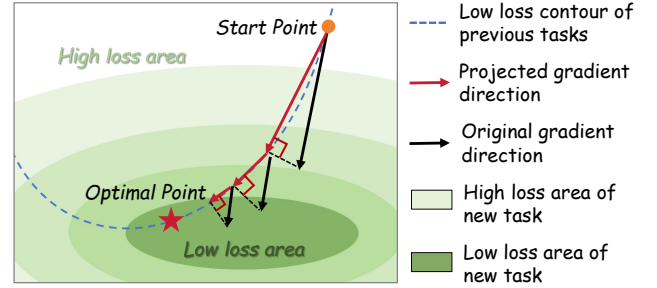


Figure 1: Orthogonal Gradient Projection (OGP) projects the original gradient of new task (black arrow) onto the null space of previous tasks, and updates model using the projected gradient (red arrow) without compromising the performance on previous tasks.

updates often inadvertently pull the originally well-aligned visual and language feature vectors in divergent directions, distorting the overall geometry of the embedding space. It is important to not only ensure the performance of downstream tasks, but also to maintain the zero-shot generalization, *i.e.*, keeping the embedding space from drifting. However, recent studies (Zheng et al. 2023; Lu et al. 2024b; Qiao et al. 2024; Yu et al. 2024a; Wu et al. 2025; Tang et al. 2024) mostly focused on the performance of downstream tasks, using methods such as knowledge distillation, prompt-tuning, Mixture-of-Expert, and synthetic data to overcome catastrophic forgetting, but little attention is paid to the relationship between changes of shared embedding space and model generalization ability.

Liang et al. (2022) has identified “modality gap”, the phenomenon where visual and language embeddings have a significant distance from each other, occupying separate conical subspaces. It is considered as an inherent characteristic of contrastively trained VLMs, related to contrastive learning loss and imbalanced modality information content (Liang et al. 2022; Jiang et al. 2023; Schrodi et al. 2025). From the perspective of modality gap, the drift of shared embedding space in continual fine-tuning manifests as a rapid change. While not a direct cause of performance decline, sharp variations of this gap serve as an effective indicator of unstable inter-modal relationships and correlate with the

degradation of zero-shot ability. Consequently, maintaining a stable modality gap is considered beneficial for preserving the model’s generalization (Liang et al. 2022; Jiang et al. 2023; Schrodi et al. 2025).

To address these challenges, we propose Gradient Null Space Projection (GNSP), an efficient continual learning method designed specifically for VLMs. Our approach is built on the principle of Orthogonal Gradient Projection (OGP) (Lopez-Paz and Ranzato 2017; Chaudhry et al. 2018; Zeng et al. 2019; Saha, Garg, and Roy 2021; Wang et al. 2021; Liang and Li 2023; Yang et al. 2025), a powerful strategy that constrains parameter updates to be orthogonal to the knowledge learned from previous tasks, as shown in Fig. 1. By projecting task-specific gradients onto the null space of previously learned knowledge, GNSP mathematically prevents interference with prior tasks, effectively mitigating catastrophic forgetting without relying on data rehearsal or architectural modifications. To preserve the global structure of the embedding space and CLIP’s zero-shot generalization, we introduce Contrastive Distillation (CD) and Modality Alignment Preservation (MAP) loss as complementary strategies. CD, using CLIP model without any fine-tuning as a teacher model and samples from ImageNet (Deng et al. 2009) as reference data to retain the original CLIP’s feature distribution. MAP loss mimics CLIP’s pre-training objective on reference data, further stabilizing the inter-modality alignment during fine-tuning. The synergy between these components is key: GNSP isolates and preserves prior task knowledge, while CD and MAP preserve the foundational VLMs generalization.

Our main contributions are:

- We propose GNSP, an orthogonal gradient projection method for VLMs continual fine-tuning that effectively prevents interference with previous tasks and overcomes catastrophic forgetting.
- We propose the modality alignment preservation to combine with contrastive distillation to approximate the pre-training data and loss of CLIP, successfully maintaining stability of the shared embedding space and zero-shot generalization.
- Our method achieved state-of-the-art performance on the MTIL benchmark, and, through the analysis of modality gap, we demonstrate its effectiveness in preserving a robust vision-language space throughout continual fine-tuning process.

2 Related Works

Continual Learning in VLMs. Pre-trained Vision-Language models are often fine-tuned for downstream tasks, and methods can be broadly grouped into three principal categories based on how they mitigate catastrophic forgetting while acquiring new knowledge. **Replay strategies** retain previous information by reusing earlier model components or stored data (Yan et al. 2022; Lei et al. 2023; Zhang, Zhang, and Xu 2023; Chen et al. 2023). **Cross-modality regularization strategies** preserves consistency between old and new tasks through alignment constraints (Zheng et al. 2023; Zhu et al. 2023; Cui et al. 2024; Yu et al. 2024b;

Lao et al. 2023). **Parameter-efficient adaptation strategies** introduce lightweight modules for low-overhead learning. This includes adapter-based methods (Jha, Gong, and Yao 2024; Liu, Zhu, and Tian 2025), low-rank decomposition (Lu et al. 2024a; Tang et al. 2024), mixture-of-experts (Yu et al. 2024a; Guo et al. 2025) and prompt-based technique (Wang, Huang, and Hong 2022; D’Alessandro et al. 2023). These methods have made significant progress in addressing catastrophic forgetting, but pay little attention to changes in modality space, which is the key to generalization.

Orthogonal gradient projection (OGP) for CL. OGP preserves prior knowledge by enforcing gradient updates for new tasks to be orthogonal to key directions of previous ones, offering strong explainability and efficiency for continual learning. While early works applied OGP in unimodal settings with CNNs (Lopez-Paz and Ranzato 2017; Zeng et al. 2019; Saha, Garg, and Roy 2021; Wang et al. 2021), recent methods extend it to prompt tuning in ViTs (Lu et al. 2024b; Qiao et al. 2024) and model editing in LLMs (Fang et al. 2025). We leverage OGP to preserve the output of model to previous tasks, maintaining the shared embedding space and cross-modal alignment of VLMs, and analyze its effectiveness from the perspective of modality gap.

Modality Gap. Multi-modal models map inputs from different modalities into a shared embedding space, but Liang et al. (2022) found that CLIP’s visual embeddings and language embeddings are located in two separate subspace of the shared embedding space, and other multi-modal models also exhibit similar phenomena. Modality gap is considered an inherent characteristic of multi-modal models, rather than a bug. It comes from nonlinear activation functions, contrastive learning loss, and imbalanced modality information (Liang et al. 2022; Schrodi et al. 2025). Previous studies (Ni et al. 2023; Yang et al. 2024; Mistretta et al. 2025) have found that when fine-tuning CLIP, the drift of embedding manifests as intra-modal drift and inter-modal rotation, and many methods have been proposed to maintain the stability of shared embedding space. We analyzed the changes in modality gap during the fine-tuning process and emphasized that maintaining this gap is necessary for better preserving the original shared embedding space.

3 Method

3.1 Preliminaries

Continual Learning Setup. We consider a standard continual learning setup where the model is trained sequentially on a series of T tasks. For a VLM like CLIP, task i consists of N^i image-text pairs $\{(I_j^{(i)}, T_j^{(i)})\}_{j=1}^{N^{(i)}}$. The objective is to adapt the model to each new task without access to data from previous ones (van de Ven and Tolias 2019), while maintaining performance across all tasks seen so far. We evaluate our method in both Task-Incremental Learning (TIL), where tasks come from different datasets, and Class-Incremental Learning (CIL), where tasks are splits of the same dataset.

Vision-Language Models. Our method is built upon CLIP (Radford et al. 2021), which comprises an image encoder and a text encoder that embed images and texts into a

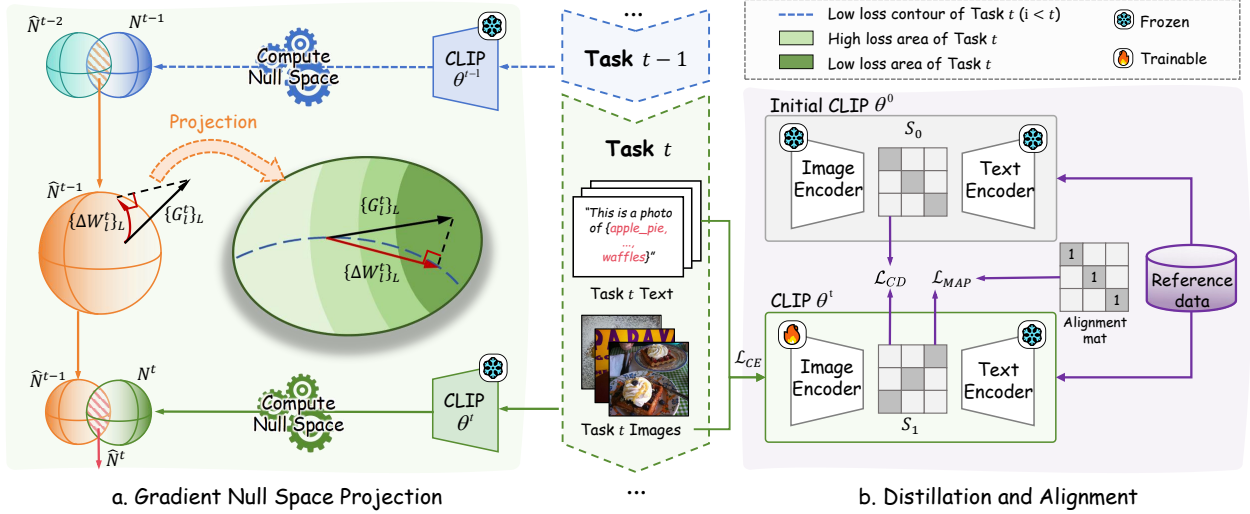


Figure 2: Framework overview of GNSP. (a) **Gradient Null Space Projection**. The updated gradient G_l^t will be projected onto the shared null space $\hat{\mathcal{N}}^{t-1}$ of previous tasks to obtain ΔW_l^t to update CLIP θ^t . After training task t , the null space \mathcal{N}^t will be computed to update the shared null space; (b) **Distillation and Alignment**. Contrastive Distillation \mathcal{L}_{CD} is used for matching CLIP θ^t and Initial CLIP θ^0 on reference data, while using MAP loss \mathcal{L}_{MAP} to preserve the modality alignment of CLIP θ^t .

shared embedding space. The probability of a text description T_j matching an image I is computed via a softmax over cosine similarities:

$$p(T_j|I) = \frac{\exp(\cos(f(I), f(T_j))/\tau)}{\sum_k \exp(\cos(f(I), f(T_k))/\tau)}, \quad (1)$$

where $f(\cdot)$ denotes the CLIP model, $\cos(\cdot, \cdot)$ denotes cosine similarity, τ is a learnable temperature parameter. For downstream classification, each category y_j is converted into a natural language prompt such as “a photo of a {object}”, and the class with the highest similarity score is the prediction of the image, and cross-entropy loss is used between the ground-truth class and the predicted probability.

3.2 Gradient Null Space Projection

To prevent catastrophic forgetting, our primary goal is to update the model for the current task t in such a way that its outputs for all previous tasks i ($i < t$) remain unchanged. We achieve this by constraining the gradient updates to the null space of previous tasks feature activations.

Formalizing the Null-Space Constraint. Consider the l -th layer of a model with weight matrix W_l^{t-1} after training on task $t-1$. Let $X_l^{t-1} \in \mathbb{R}^{N_i \times d}$ denote the input activation matrix at l -th layer when processing data from previous task $t-1$. The l -th layer’s output is:

$$O_l^{t-1} = X_l^{t-1} W_l^{t-1} + b_l^{t-1}, \quad (2)$$

$$X_{l+1}^{t-1} = \sigma(O_l^{t-1}), \quad (3)$$

where $\sigma(\cdot)$ is a nonlinear activation function, and we freeze the bias term b_l^{t-1} . During training on current task t , the updated weight becomes $W_l^t = W_l^{t-1} + \Delta W_l^t$. We denote

\mathcal{N}_l^{t-1} as the null space of X_l^{t-1} , and if this update lies in it, we have:

$$X_l^{t-1} \Delta W_l^t = 0, \quad (4)$$

then the layer’s output for task $t-1$ remains invariant:

$$O_l^t = X_l^{t-1} W_l^t + b_l^t = O_l^{t-1}. \quad (5)$$

Similarly, if W_l^{t-1} is located in the common null space $\hat{\mathcal{N}}_l^{t-1}$ of all previous tasks, i.e., $\hat{\mathcal{N}}_l^{t-1} = \bigcap_{i=1}^{t-1} \mathcal{N}_l^i$, the model’s behavior on all previous tasks will be preserved.

The constraint in Eq.4 is the core of our approach and ensures that parameter updates for a new task are performed in a subspace that is orthogonal to the features of the previous tasks. As a result, the geometric structure of the embedding space established by the prior knowledge is mathematically preserved. We need to project the original gradient into the common null space $\hat{\mathcal{N}}^{t-1}$ to obtain ΔW^t that satisfies Eq.4.

Adaptive Construction of the Projection Matrix. Obtaining the projection matrix requires the activation feature matrices X_l^{t-1} , but directly storing X_l^i for all previous tasks i is impractical due to memory constraints, especially when N^i is large. Instead, we compute the gram matrix:

$$M_l^{t-1} = \frac{(X_l^{t-1})^\top X_l^{t-1}}{\|(X_l^{t-1})^\top X_l^{t-1}\|_F} \in \mathbb{R}^{d \times d}, \quad (6)$$

where $\|\cdot\|_F$ represents Frobenius norm. It can be proved that M_l^{t-1} shares the same right null space as X_l^{t-1} . To get the common null space $\hat{\mathcal{N}}_l^{t-1}$, we accumulate the covariance matrices:

$$\hat{M}_l^{t-1} = \sum_{i=1}^{t-1} M_l^i, \quad (7)$$

then the null space of \hat{M}_l^{t-1} represents the common null space of all previous task features. We find this null

space \hat{N}_l^{t-1} via Singular Value Decomposition (SVD), $U, \Sigma, V^\top = \text{SVD}(\hat{M}_l^{t-1})$, where $V \in \mathbb{R}^{d \times d}$ contains the right singular vectors, and $\Sigma = \text{diag}(\sigma_1, \sigma_2, \dots, \sigma_d)$ with $\sigma_1 \geq \sigma_2 \geq \dots \geq \sigma_d \geq 0$. Set a singular value threshold σ_m , partitioning Σ and V into $\Sigma = \begin{bmatrix} \Sigma_1 & 0 \\ 0 & \Sigma_2 \end{bmatrix}$, $V = [V_1, V_2]$, all singular value of Σ_2 are smaller than σ_m , and V_2 contains the singular vectors corresponding to singular values Σ_2 . The projection matrix is defined as:

$$P_l^{t-1} = V_2 V_2^\top. \quad (8)$$

If $\sigma_m = 0$, it means that all column vectors of V_2 are bases of the null space of \hat{M}_l^{t-1} , P_l^{t-1} projects any update onto the common null space \hat{N}_l^{t-1} .

In practice, the singular values of each FFN gram matrix in CLIP are almost all non-zero and exhibits an extreme long-tail distribution, as Fig.3 shows. Directly setting $\sigma_m = 0$ yields an extremely low-rank projection matrix, hindering the model’s ability to learn new tasks. Previous works (Wang et al. 2021; Lopez-Paz and Ranzato 2017; Saha, Garg, and Roy 2021; Fang et al. 2025), use fixed small thresholds or preset projection dimensions (e.g., $d/2$) to approximate the null space. Instead, we adopt an adaptive strategy: σ_m is chosen such that the sum of singular values below it accounts for no more than a fixed ratio ρ (e.g., 15%) of the total spectrum:

$$\sum_{\sigma_i \leq \sigma_m} \sigma_i \leq \rho \cdot \sum_{\text{all}} \sigma_j. \quad (9)$$

This adaptive strategy automatically fits the spectral distribution of each layer, balancing knowledge preservation and model plasticity without manual threshold tuning.

Update with Projected Gradients. For the current task t , we first compute the original gradient G_l^t for layer l . The final update is then obtained by projecting this gradient onto the computed null space:

$$\Delta W_l^t = P_l^{t-1} G_l^t, \quad (10)$$

which guarantees that Eq.4 holds true, and ensuring the output for previous tasks remains invariant and preventing catastrophic forgetting. Since the projection only requires gram matrices of intermediate features, the memory cost remains constant across tasks.

Detail proof about this subsection can be found in supplementary.

3.3 Contrastive Distillation

GNSP effectively preserves performance on learned tasks, but it does not explicitly maintain the rich, general-purpose structure of CLIP’s original embedding space, which is the source of its zero-shot generalization. To address this, we employ Knowledge Distillation (KD) (Hinton, Vinyals, and Dean 2015), using the initial, pre-trained CLIP model as a teacher to guide the student model. Following the Contrastive Distillation (CD) (Wu et al. 2025) framework, we encourage the student model to replicate the teacher’s image-to-text and text-to-image similarity structures. We

use ImageNet (Deng et al. 2009) dataset, which is close to CLIP’s pretraining datas, and select 1000 randomly sampled images from ImageNet as reference data, striking a good balance between effectiveness and efficiency. For a batch of B image-text pairs $\{(I_i, T_i)\}_{i=1}^B$ from reference data, let S^0 and $S^t \in \mathbb{R}^{B \times B}$ denote the cosine similarity matrices computed by the teacher f^0 and student model f^t , respectively:

$$S_{i,j}^0 = \cos(f^0(I_i), f^0(T_j)), \quad (11)$$

$$S_{i,j}^t = \cos(f^t(I_i), f^t(T_j)), \quad (12)$$

then scale the similarity matrices by a temperature factor τ to obtain the logits:

$$Z^0 = \frac{S^0}{\tau}, \quad Z^t = \frac{S^t}{\tau}. \quad (13)$$

We compute row-wise (image-to-text alignment) and column-wise (text-to-image alignment) KL divergence:

$$\mathcal{L}_{\text{KD_I2T}} = \sum_{i=1}^B \text{KL}(\text{softmax}(Z_{i,:}^0) \parallel \text{softmax}(Z_{i,:}^t)), \quad (14)$$

$$\mathcal{L}_{\text{KD_T2I}} = \sum_{j=1}^B \text{KL}(\text{softmax}(Z_{:,j}^0) \parallel \text{softmax}(Z_{:,j}^t)). \quad (15)$$

The final Contrastive Distillation loss is:

$$\mathcal{L}_{\text{CD}} = \mathcal{L}_{\text{KD_I2T}} + \mathcal{L}_{\text{KD_T2I}}. \quad (16)$$

3.4 Modality Alignment Preservation

While distillation aligns the output similarity matrices, we can further stabilize the embedding space by enforcing a feature-level constraint that mimics CLIP’s original contrastive pre-training objective. We propose the Modality Alignment Preservation (MAP) loss, which computes a standard in-batch contrastive loss on the reference data. For a batch of B image-text pairs, the symmetric loss is:

$$\mathcal{L}_{\text{MAP_I2T}} = -\frac{1}{B} \sum_{i=1}^B \log \frac{\exp(Z_{t_i,i})}{\sum_{j=1}^B \exp(Z_{t_i,j})}, \quad (17)$$

$$\mathcal{L}_{\text{MAP_T2I}} = -\frac{1}{B} \sum_{i=1}^B \log \frac{\exp(Z_{t_i,i})}{\sum_{j=1}^B \exp(Z_{t_j,i})}. \quad (18)$$

The final Modality Alignment Preservation loss is:

$$\mathcal{L}_{\text{MAP}} = \mathcal{L}_{\text{MAP_I2T}} + \mathcal{L}_{\text{MAP_T2I}}. \quad (19)$$

3.5 Overall Training Objective

The final training loss for each task is a weighted sum of the three components:

$$\mathcal{L} = \mathcal{L}_{\text{CE}} + \lambda \cdot \mathcal{L}_{\text{CD}} + \beta \cdot \mathcal{L}_{\text{MAP}}, \quad (20)$$

here, \mathcal{L}_{CE} is the standard cross-entropy loss for the current task, driving adaptation. \mathcal{L}_{CD} and \mathcal{L}_{MAP} act as regularization terms on the reference data to preserve generalization and alignment.

The entire optimization is constrained by our GNSP mechanism, which projects the final gradient into the null space of past knowledge before the weight update. This multi-faceted approach allows the model to learn new information effectively while robustly preserving both past-task knowledge and foundational zero-shot capabilities.

Table 1: Comparison of SOTA methods on MTIL Order I.

Method	<i>Transfer</i>	<i>Avg</i>	<i>Last</i>
Zero-shot	69.4	65.3	65.3
Continual Fine-tune	49.9	52.1	69.2
LwF (Li and Hoiem 2017)	56.9	64.7	74.6
Wise-FT (Wortsman et al. 2022)	52.3	60.7	77.7
ZSCL (Zheng et al. 2023)	68.1	75.4	83.6
MoE-Adapter (Yu et al. 2024a)	68.9	76.7	85.0
AwoForget (Zheng et al. 2024)	69.8	<u>76.9</u>	85.1
DIKI (Tang et al. 2024)	68.7	76.3	85.1
GIFT (Wu et al. 2025)	<u>69.3</u>	77.3	86.0
Ours	68.9	77.3	86.4

4 Experiments

4.1 Experiments Setting

Model and Benchmarks All experiments are conducted using the CLIP ViT-B/16 model. We evaluate on two primary continual learning benchmarks. For Task-Incremental Learning, we use the MTIL benchmark proposed by (Zheng et al. 2023), which consists of 11 diverse datasets (Maji et al. 2013; Fei-Fei, Fergus, and Perona 2004; Krizhevsky and Hinton 2009; Cimpoi et al. 2014; Helber et al. 2019; Nilsback and Zisserman 2008; Bossard, Guillaumin, and Van Gool 2014; Deng 2012; Parkhi et al. 2012; Krause et al. 2013; Xiao et al. 2010). We follow two official task orderings, with Order II (where the simple MNIST dataset is introduced early) serving as our primary setting to reduce its outsized impact on later tasks. For Class-Incremental Learning, we use the CIFAR100 (Krizhevsky and Hinton 2009) and TinyImageNet (Yan, Xie, and He 2021) datasets, following standard protocols (Douillard et al. 2021). Details and experimental results can be found in supplementary.

Metrics For MTIL benchmark, we report on three key metrics: 1) *Last* accuracy, which measures performance on previously seen tasks to evaluate knowledge retention; 2) *Transfer* accuracy, which assesses zero-shot performance on unseen tasks to gauge generalization; and 3) *Average* accuracy, a composite metric reflecting overall performance throughout the continual learning process. For CIL (Douillard et al. 2021), we report the standard *Average* accuracy across all learned classes.

Implementation Details We fine-tune the 12 Feed-Forward Network (FFN) layers within the image encoder, as they are widely considered to store task-specific knowledge (Hase et al. 2023; Geva et al. 2021; Fang et al. 2025). For each MTIL task, we train for 500-1000 iterations with a batch size of 64. Key hyperparameters are set as follows: the singular value ratio for the GNSP null space $\rho = 0.15$, and loss hyper-parameters $\lambda = 1$, $\beta = 0.75$. Further details are available in supplementary.

4.2 Main Results on MTIL

As shown in Tab.1 and Tab.2, our method establishes a new state-of-the-art on the MTIL benchmark across both task or-

Table 2: Comparison of SOTA methods on MTIL Order II.

Method	<i>Transfer</i>	<i>Avg</i>	<i>Last</i>
Zero-shot	65.4	65.3	65.3
Continual Fine-tune	56.5	59.9	63.0
LwF (Li and Hoiem 2017)	53.2	62.2	71.9
Wise-FT (Wortsman et al. 2022)	51.0	61.5	72.2
ZSCL (Zheng et al. 2023)	64.2	74.5	83.4
MoE-Adapter (Yu et al. 2024a)	64.3	74.7	84.1
AwoForget (Zheng et al. 2024)	65.4	<u>75.9</u>	<u>85.4</u>
DIKI (Tang et al. 2024)	64.4	74.5	85.5
GIFT (Wu et al. 2025)	65.9	75.7	85.3
Ours	<u>65.7</u>	76.7	87.7

derings. 1) Forgetting Prevention: GNSP achieves the highest *Last* accuracy, demonstrating its superior ability to mitigate catastrophic forgetting. Notably, under Order II, it surpasses the previous best method by a significant 2.3% margin. This result directly validates the effectiveness of our core Gradient Null-Space Projection mechanism in protecting knowledge from previously learned tasks; 2) Generalization Preservation: Our method’s *Transfer* accuracy remains remarkably close to the Zero-shot CLIP upper bound and is competitive with the top-performing methods. This confirms that our knowledge distillation and modality alignment strategies successfully preserve CLIP’s intrinsic zero-shot generalization capabilities; 3) Overall Performance: GNSP also achieves the highest *Average* accuracy, indicating that it strikes the most effective balance between stability (retaining past and general knowledge) and plasticity (learning new tasks).

4.3 Ablation Studies

To dissect the contributions of our method’s components and the impact of key hyperparameters, we conducted extensive ablation studies on the MTIL Order II benchmark.

Table 3: Ablation on different components.

Method			<i>Transfer</i>	<i>Avg</i>	<i>Last</i>
Zero-shot			65.4	65.3	65.3
Continual Fine-tune			44.6	55.9	77.3
+GNSP	+CD	+MAP	<i>Transfer</i>	<i>Avg</i>	<i>Last</i>
	✓		64.0	72.7	80.7
✓			61.4	73.4	86.5
✓	✓		65.2	76.4	87.5
✓	✓	✓	65.7	76.7	87.7

Impact of Individual Components. We progressively added each component to a standard continual fine-tune baseline with only FFN layers of image-encoder are trainable, and results are presented in Tab.3. **GNSP** alone significantly improves the *Last* metric, confirming its role in

Table 4: Ablation study on hyperparameter choices. Default settings are marked by underline, which uses $\rho = 0.15$ for GNSP, Initial CLIP and 1k ImageNet images for CD, $\beta = 0.75$ for MAP.

Hyperparameters		<i>Transfer</i>	<i>Avg</i>	<i>Last</i>
(a) ρ	0.1	65.73	76.48	86.98
	<u>0.15</u>	65.72	76.67	87.65
	0.2	65.66	76.62	87.50
(b) Souore	current	64.73	73.93	83.35
	ImageNet	65.72	76.67	87.65
	Synthetic(1k)	64.49	75.32	86.45
(c) Teacher	<u>CLIP</u>	65.72	76.67	87.65
	Last	65.43	76.42	87.36
	WISE(0.5)	65.47	76.36	87.25
(d) Number	0.5k	64.69	75.89	87.52
	<u>1k</u>	65.72	76.67	87.65
	10k	65.09	75.77	86.84
(e) β	0.5	65.60	76.55	87.34
	<u>0.75</u>	65.72	76.67	87.65
	1.0	65.60	76.55	87.42

knowledge retention, but *Transfer* performance degrades without a mechanism to preserve the original embedding space. **CD** alone excels in preserving *Transfer* performance by mimicking the initial CLIP model, but suffers from forgetting, as shown by a lower *Last* score. The combination of GNSP and CD yields a powerful synergistic effect, surpassing prior SOTA methods on both *Average* and *Last* while maintaining high *Transfer* performance. Adding Modality **MAP** provides a final boost to all metrics, achieving our best results by further stabilizing the shared embedding space.

Gradient Null Space Projection. ρ controls singular value threshold σ_m , which determines the rank of the projection matrix. Fig.3 shows the curves of singular values of gram matrix M_l^0 of some FFN layers in CLIP. The singular values smaller than σ_m are colored in orange. A larger ρ resulting in a higher-dimensional null space and allowing updates in more directions to enhance the model’s plasticity. As Tab.4(a) shows, a larger ρ improves *Last*, while the *Transfer* gradually decreases. When ρ is too large (larger than 0.2), forgetting also occurs, result in a decrease in *Last*.

Contrastive Distillation. The selection of reference data and teacher models is a key factor in Contrastive Distillation, as shown in Tab.4(b) and Tab.4(c). The Synthetic (1k) refers to the 1k images synthesized from Stable Diffusion(Wu et al. 2025). The combination of ImageNet and CLIP achieved the best results. In the selection of teacher models, Last is only slightly lower than CLIP, which is also due to our method maintaining the performance of last well and avoiding the accumulation of errors. In terms of the number of reference images, 1k images achieved the best results in Tab.4(d), while too many images can actually damage the performance of the model.

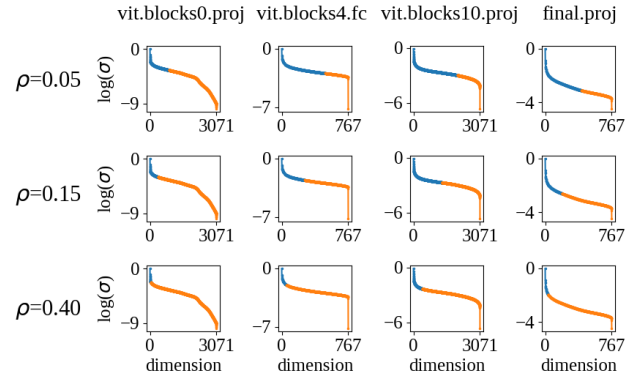


Figure 3: Singular values of gram matrix at different layers of initial CLIP on 100k images from ImageNet. The singular values smaller than σ_m are colored in orange. As ρ increases, the number of selected singular values increases, and the dimension of null space also becomes higher. Note that logarithmic values in vertical axis.

Modality Alignment Preservation. From the Tab.4(e), it can be seen that regardless of the value of β between 0 and 1, the performance of model is improved, and the best performance is achieved when $\beta = 0.75$, indicating that the model can fit well in fine-tuned datasets while preserve modality alignment.

4.4 Analysis on Modality Gap

We conducted continual fine-tuning under the Order II setting of MTIL, randomly selecting 200 images from the test set for each dataset, and also randomly selecting 2000 image-text pairs from COCO Captions (Chen et al. 2015) as external data references. For each paired image-text pair (I_i, T_i) in the dataset, we calculate the modality gap Δ_{gap} by:

$$\Delta_{gap} = \frac{1}{N} \sum_{i=1}^N \cos(f(I_i), f(T_i)). \quad (21)$$

Fig.4 shows the changes in modality gap of Continual Fine-tune, GIFT (Wu et al. 2025), Ours and Ours without MAP during the continual fine-tuning process. The vertical dashed line represents the fine-tuning position of this dataset in MTIL Order II. It can be seen that all these datasets have undergone significant changes before and after fine-tuning, indicating that fine-tuning can change the alignment between image and text in this domain, while it also affects the alignment in other domains. Taking Food dataset Fig.4(b) as an example, when fine-tuning other datasets (task 3-11), the Continual Fine-tune method exhibits severe fluctuations, while the GIFT method continues to increase, indicating that these methods cause significant damage to the shared embedding space. However, our method remains relatively stable. With MAP component, the modality gap is further stabilized, demonstrating the effectiveness of our method in maintaining the shared embedding space. Although these methods may appear good in MTIL evalua-

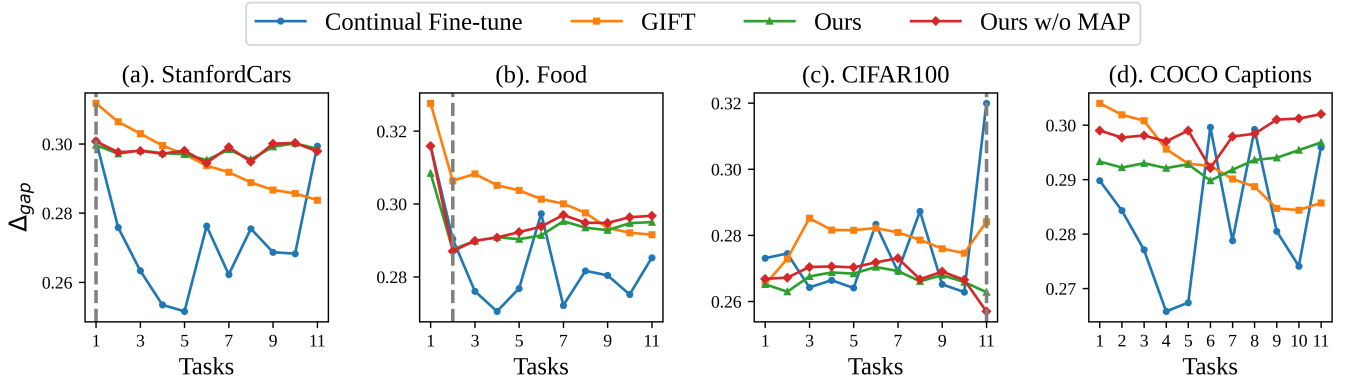


Figure 4: The variation of modality gap when fine-tuning using different methods, with the vertical dashed line representing the fine-tuning position. All have undergone significant changes before and after fine-tuning. Throughout the entire fine-tuning process, the Continual Fine-tune and GIFT show significant fluctuations, while Ours maintains the gap most stably.

Table 5: Image-to-Text Retrieval *Recall@k* on COCO Captions.

Method	<i>R@1</i>	<i>R@5</i>	<i>R@10</i>
Zero-shot	29.9	50.7	60.2
Continual Fine-tune	9.0	20.7	28.0
GIFT (Wu et al. 2025)	28.1	48.9	58.0
Ours	29.0	49.7	59.1

tion metrics, they **implicitly** disrupt the shared embedding space during fine-tuning, causing drastic changes in modality gaps, leading to degradation in other cross-modal tasks. We performed image-to-text retrieval on COCO Captions (Chen et al. 2015), as shown in Tab.5. Compared to the Zero-shot results, other methods have a significant decrease in retrieval accuracy due to the destruction of shared embedding space, while our method shows the smallest. This result confirms that during the continual fine-tuning process, changes in modality gaps can lead to a decrease in generalization, and **maintaining the stability of modality spatial structure is crucial to the continual learning for Vision-Language Models**.

Fig.5 shows the t-SNE (van der Maaten and Hinton 2008) visualization of visual features. It can be clearly observed that simple continual fine-tuning leads to significant feature drift, corresponding to the overall drift of the visual subspace. At the same time, language subspaces also drift, disrupting modality alignment and causing drastic changes in modality gaps, resulting in a sharp decline in performance. Our method showed almost no drift on StanfordCars and only slight drift on COCO Captions without changing the spatial structure, confirming the ability to maintain feature invariance. Whether it is knowledge of fine-tuning tasks or pre-trained knowledge, using our method for fine-tuning can effectively prevent forgetting.

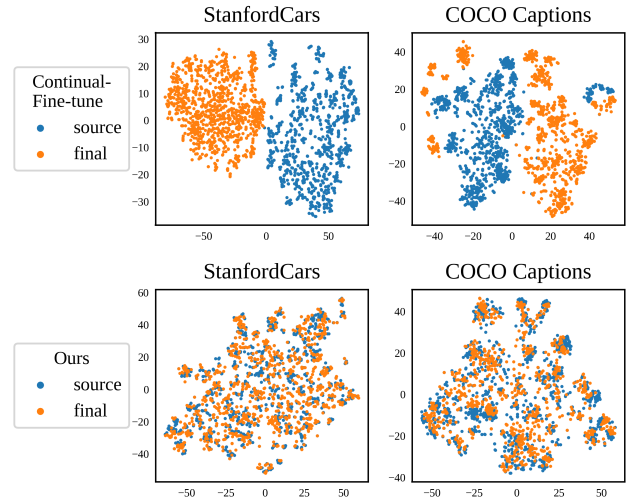


Figure 5: T-SNE visualization. For StanfordCars, “source” is extracted from the model just fine-tuned, For COCO Captions, “source” is taken from original CLIP. Both “final” come from the model fine-tuned on all datasets. The Continual Fine-tune has experienced significant overall drift, while Ours has effectively maintained features unchanged.

5 Conclusion

We propose a continual fine-tuning method for Vision-Language Models. The core includes three parts: Gradient Null Space Projection, Contrastive Distillation, and Modality Alignment Preservation. GNSP updates the model by projecting gradients onto the null space of previous knowledge. CD aligns the output distribution of current model with CLIP, MAP preserves the stability of shared embedding space. The experiment results show that our method achieves excellent performance on MTIL benchmark, while maintaining stable modality gap, preserving the shared embedding space of original CLIP, and maintaining the generalization on other cross-modal tasks.

References

- Bossard, L.; Guillaumin, M.; and Van Gool, L. 2014. Food-101 – Mining Discriminative Components with Random Forests. In Fleet, D.; Pajdla, T.; Schiele, B.; and Tuytelaars, T., eds., *Computer Vision – ECCV 2014*, 446–461. Cham: Springer International Publishing.
- Chaudhry, A.; Ranzato, M.; Rohrbach, M.; and Elhoseiny, M. 2018. Efficient Lifelong Learning with A-GEM. *arXiv:1812.00420*.
- Chen, X.; Fang, H.; Lin, T.-Y.; Vedantam, R.; Gupta, S.; Dollár, P.; and Zitnick, C. L. 2015. Microsoft coco captions: Data collection and evaluation server. *arXiv preprint arXiv:1504.00325*.
- Chen, X.; Zhang, J.; Wang, X.; Zhang, N.; Wu, T.; Wang, Y.; Wang, Y.; and Chen, H. 2023. Continual multimodal knowledge graph construction. *arXiv preprint arXiv:2305.08698*.
- Cimpoi, M.; Maji, S.; Kokkinos, I.; Mohamed, S.; and Vedaldi, A. 2014. Describing Textures in the Wild. In *2014 IEEE Conference on Computer Vision and Pattern Recognition*, 3606–3613.
- Cui, Z.; Peng, Y.; Wang, X.; Zhu, M.; and Zhou, J. 2024. Continual vision-language retrieval via dynamic knowledge rectification. In *Proceedings of the AAAI Conference on Artificial Intelligence*, volume 38, 11704–11712.
- D’Alessandro, M.; Alonso, A.; Calabrés, E.; and Galar, M. 2023. Multimodal parameter-efficient few-shot class incremental learning. In *Proceedings of the IEEE/CVF International Conference on Computer Vision*, 3393–3403.
- Deng, J.; Dong, W.; Socher, R.; Li, L.-J.; Li, K.; and Fei-Fei, L. 2009. Imagenet: A large-scale hierarchical image database. In *2009 IEEE conference on computer vision and pattern recognition*, 248–255. Ieee.
- Deng, L. 2012. The MNIST Database of Handwritten Digit Images for Machine Learning Research [Best of the Web]. *IEEE Signal Processing Magazine*, 29(6): 141–142.
- Douillard, A.; Rame, A.; Couairon, G.; and Cord, M. 2021. DyTox: Transformers for Continual Learning with DYnamic TOken eXpansion. In *Proceedings of the IEEE/CVF Conference on Computer Vision and Pattern Recognition*.
- Fang, J.; Jiang, H.; Wang, K.; Ma, Y.; Shi, J.; Wang, X.; He, X.; and Chua, T.-S. 2025. AlphaEdit: Null-Space Constrained Knowledge Editing for Language Models. In *The Thirteenth International Conference on Learning Representations*.
- Fei-Fei, L.; Fergus, R.; and Perona, P. 2004. Learning Generative Visual Models from Few Training Examples: An Incremental Bayesian Approach Tested on 101 Object Categories. In *2004 Conference on Computer Vision and Pattern Recognition Workshop*, 178–178.
- Geva, M.; Schuster, R.; Berant, J.; and Levy, O. 2021. Transformer Feed-Forward Layers Are Key-Value Memories. In *Proceedings of the 2021 Conference on Empirical Methods in Natural Language Processing*. Association for Computational Linguistics.
- Goodfellow, I. J.; Mirza, M.; Xiao, D.; Courville, A.; and Bengio, Y. 2013. An empirical investigation of catastrophic forgetting in gradient-based neural networks. *arXiv:1312.6211*.
- Guo, H.; Zeng, F.; Xiang, Z.; Zhu, F.; Wang, D.-H.; Zhang, X.-Y.; and Liu, C.-L. 2025. Hide-llava: Hierarchical decoupling for continual instruction tuning of multimodal large language model. *arXiv preprint arXiv:2503.12941*.
- Hase, P.; Bansal, M.; Kim, B.; and Ghandeharioun, A. 2023. Does localization inform editing? surprising differences in causality-based localization vs. knowledge editing in language models. *Advances in Neural Information Processing Systems*, 36: 17643–17668.
- Helber, P.; Bischke, B.; Dengel, A.; and Borth, D. 2019. EuroSAT: A Novel Dataset and Deep Learning Benchmark for Land Use and Land Cover Classification. *IEEE Journal of Selected Topics in Applied Earth Observations and Remote Sensing*, 12(7): 2217–2226.
- Hinton, G.; Vinyals, O.; and Dean, J. 2015. Distilling the knowledge in a neural network. *arXiv:1503.02531*.
- Jha, S.; Gong, D.; and Yao, L. 2024. Clap4clip: Continual learning with probabilistic finetuning for vision-language models. *Advances in neural information processing systems*, 37: 129146–129186.
- Jia, C.; Yang, Y.; Xia, Y.; Chen, Y.-T.; Parekh, Z.; Pham, H.; Le, Q. V.; Sung, Y.-H.; Li, Z.; and Duerig, T. 2021. Scaling Up Visual and Vision-Language Representation Learning With Noisy Text Supervision. In *International Conference on Machine Learning*.
- Jiang, Q.; Chen, C.; Zhao, H.; Chen, L.; Ping, Q.; Tran, S. D.; Xu, Y.; Zeng, B.; and Chilimbi, T. 2023. Understanding and constructing latent modality structures in multi-modal representation learning. In *Proceedings of the IEEE/CVF Conference on Computer Vision and Pattern Recognition*, 7661–7671.
- Kirkpatrick, J.; Pascanu, R.; Rabinowitz, N. C.; Veness, J.; Desjardins, G.; Rusu, A. A.; Milan, K.; Quan, J.; Ramalho, T.; Grabska-Barwinska, A.; Hassabis, D.; Clopath, C.; Kumaran, D.; and Hadsell, R. 2016. Overcoming catastrophic forgetting in neural networks. *Proceedings of the National Academy of Sciences*, 114: 3521 – 3526.
- Krause, J.; Stark, M.; Deng, J.; and Fei-Fei, L. 2013. 3D Object Representations for Fine-Grained Categorization. In *2013 IEEE International Conference on Computer Vision Workshops*, 554–561.
- Krizhevsky, A.; and Hinton, G. 2009. Learning multiple layers of features from tiny images. *Handbook of Systemic Autoimmune Diseases*, 1(4).
- Lao, M.; Pu, N.; Liu, Y.; Zhong, Z.; Bakker, E. M.; Sebe, N.; and Lew, M. S. 2023. Multi-domain lifelong visual question answering via self-critical distillation. In *Proceedings of the 31st ACM International Conference on Multimedia*, 4747–4758.
- Lei, S. W.; Gao, D.; Wu, J. Z.; Wang, Y.; Liu, W.; Zhang, M.; and Shou, M. Z. 2023. Symbolic replay: Scene graph as prompt for continual learning on vqa task. In *Proceedings of the AAAI Conference on Artificial Intelligence*, volume 37, 1250–1259.

- Li, Z.; and Hoiem, D. 2017. Learning without forgetting. *IEEE transactions on pattern analysis and machine intelligence*, 40(12): 2935–2947.
- Liang, W.; Zhang, Y.; Kwon, Y.; Yeung, S.; and Zou, J. 2022. Mind the Gap: Understanding the Modality Gap in Multimodal Contrastive Representation Learning. In *NeurIPS*.
- Liang, Y.-S.; and Li, W.-J. 2023. Adaptive Plasticity Improvement for Continual Learning. In *2023 IEEE/CVF Conference on Computer Vision and Pattern Recognition (CVPR)*, 7816–7825.
- Liu, W.; Zhu, F.; and Tian, Q. 2025. C-CLIP: Multimodal continual learning for vision-language model. In *The Thirteenth International Conference on Learning Representations*.
- Lopez-Paz, D.; and Ranzato, M. 2017. Gradient episodic memory for continual learning. In *Proceedings of the 31st International Conference on Neural Information Processing Systems, NIPS’17*, 6470–6479. Red Hook, NY, USA: Curran Associates Inc. ISBN 9781510860964.
- Lu, H.; Zhao, C.; Xue, J.; Yao, L.; Moore, K.; and Gong, D. 2024a. Adaptive rank, reduced forgetting: Knowledge retention in continual learning vision-language models with dynamic rank-selective lora. *arXiv preprint arXiv:2412.01004*.
- Lu, Y.; Zhang, S.; Cheng, D.; Xing, Y.; Wang, N.; Wang, P.; and Zhang, Y. 2024b. Visual prompt tuning in null space for continual learning. *Advances in neural information processing systems*, 37: 7878–7901.
- Maji, S.; Rahtu, E.; Kannala, J.; Blaschko, M. B.; and Vedaldi, A. 2013. Fine-Grained Visual Classification of Aircraft. *arXiv:1306.5151*.
- McCloskey, M.; and Cohen, N. J. 1989. Catastrophic Interference in Connectionist Networks: The Sequential Learning Problem. *Psychology of Learning and Motivation*, 24: 109–165.
- Mistretta, M.; Baldrati, A.; Agnolucci, L.; Bertini, M.; and Bagdanov, A. D. 2025. Cross the Gap: Exposing the Intra-modal Misalignment in CLIP via Modality Inversion. In *The Thirteenth International Conference on Learning Representations*.
- Ni, Z.; Wei, L.; Tang, S.; Zhuang, Y.; and Tian, Q. 2023. Continual vision-language representation learning with off-diagonal information. In *International Conference on Machine Learning*, 26129–26149. PMLR.
- Nilsback, M.-E.; and Zisserman, A. 2008. Automated Flower Classification over a Large Number of Classes. In *2008 Sixth Indian Conference on Computer Vision, Graphics & Image Processing*, 722–729.
- Parkhi, O. M.; Vedaldi, A.; Zisserman, A.; and Jawahar, C. V. 2012. Cats and dogs. In *2012 IEEE Conference on Computer Vision and Pattern Recognition*, 3498–3505.
- Qiao, J.; Tan, X.; Chen, C.; Qu, Y.; Peng, Y.; Xie, Y.; et al. 2024. Prompt gradient projection for continual learning. In *The Twelfth International Conference on Learning Representations*.
- Radford, A.; Kim, J. W.; Hallacy, C.; Ramesh, A.; Goh, G.; Agarwal, S.; Sastry, G.; Askell, A.; Mishkin, P.; Clark, J.; Krueger, G.; and Sutskever, I. 2021. Learning Transferable Visual Models From Natural Language Supervision. In *International Conference on Machine Learning*.
- Saha, G.; Garg, I.; and Roy, K. 2021. Gradient Projection Memory for Continual Learning. In *International Conference on Learning Representations*.
- Schrodi, S.; Hoffmann, D. T.; Argus, M.; Fischer, V.; and Brox, T. 2025. Two Effects, One Trigger: On the Modality Gap, Object Bias, and Information Imbalance in Contrastive Vision-Language Models. In *The Thirteenth International Conference on Learning Representations*.
- Tang, L.; Tian, Z.; Li, K.; He, C.; Zhou, H.; Zhao, H.; Li, X.; and Jia, J. 2024. Mind the interference: Retaining pre-trained knowledge in parameter efficient continual learning of vision-language models. In *European conference on computer vision*, 346–365. Springer.
- van de Ven, G. M.; and Tolias, A. S. 2019. Three scenarios for continual learning. *arXiv:1904.07734*.
- van der Maaten, L.; and Hinton, G. 2008. Visualizing Data using t-SNE. *Journal of Machine Learning Research*, 9(86): 2579–2605.
- Wang, S.; Li, X.; Sun, J.; and Xu, Z. 2021. Training networks in null space of feature covariance for continual learning. In *Proceedings of the IEEE/CVF conference on Computer Vision and Pattern Recognition*, 184–193.
- Wang, Y.; Huang, Z.; and Hong, X. 2022. S-prompts learning with pre-trained transformers: An occam’s razor for domain incremental learning. *Advances in Neural Information Processing Systems*, 35: 5682–5695.
- Wortsman, M.; Ilharco, G.; Kim, J. W.; Li, M.; Kornblith, S.; Roelofs, R.; Lopes, R. G.; Hajishirzi, H.; Farhadi, A.; Namkoong, H.; et al. 2022. Robust fine-tuning of zero-shot models. In *Proceedings of the IEEE/CVF conference on computer vision and pattern recognition*, 7959–7971.
- Wu, B.; Shi, W.; Wang, J.; and Ye, M. 2025. Synthetic Data is an Elegant GIFT for Continual Vision-Language Models. In *Proceedings of the Computer Vision and Pattern Recognition Conference*, 2813–2823.
- Xiao, J.; Hays, J.; Ehinger, K. A.; Oliva, A.; and Torralba, A. 2010. SUN database: Large-scale scene recognition from abbey to zoo. In *2010 IEEE Computer Society Conference on Computer Vision and Pattern Recognition*, 3485–3492.
- Yan, S.; Hong, L.; Xu, H.; Han, J.; Tuytelaars, T.; Li, Z.; and He, X. 2022. Generative negative text replay for continual vision-language pretraining. In *European Conference on Computer Vision*, 22–38. Springer.
- Yan, S.; Xie, J.; and He, X. 2021. DER: Dynamically Expandable Representation for Class Incremental Learning. In *Proceedings of the IEEE Conference on Computer Vision and Pattern Recognition (CVPR)*.
- Yang, E.; Shen, L.; Wang, Z.; Liu, S.; Guo, G.; Wang, X.; and Tao, D. 2025. Revisiting Flatness-Aware Optimization in Continual Learning With Orthogonal Gradient Projection. *IEEE Transactions on Pattern Analysis and Machine Intelligence*.

- Yang, Y.; Wan, F.; Jiang, Q.-Y.; and Xu, Y. 2024. Facilitating Multimodal Classification via Dynamically Learning Modality Gap. In Globerson, A.; Mackey, L.; Belgrave, D.; Fan, A.; Paquet, U.; Tomczak, J.; and Zhang, C., eds., *Advances in Neural Information Processing Systems*, volume 37, 62108–62122. Curran Associates, Inc.
- Yu, J.; Zhuge, Y.; Zhang, L.; Hu, P.; Wang, D.; Lu, H.; and He, Y. 2024a. Boosting continual learning of vision-language models via mixture-of-experts adapters. In *Proceedings of the IEEE/CVF Conference on Computer Vision and Pattern Recognition*, 23219–23230.
- Yu, Y.-C.; Huang, C.-P.; Chen, J.-J.; Chang, K.-P.; Lai, Y.-H.; Yang, F.-E.; and Wang, Y.-C. F. 2024b. Select and distill: Selective dual-teacher knowledge transfer for continual learning on vision-language models. In *European Conference on Computer Vision*, 219–236. Springer.
- Zeng, G.; Chen, Y.; Cui, B.; and Yu, S. 2019. Continual learning of context-dependent processing in neural networks. *Nature Machine Intelligence*, 1(8): 364–372.
- Zhang, X.; Zhang, F.; and Xu, C. 2023. Vqacl: A novel visual question answering continual learning setting. In *Proceedings of the IEEE/CVF Conference on Computer Vision and Pattern Recognition*, 19102–19112.
- Zheng, M.; Tang, Y.; Hao, Z.; Han, K.; Wang, Y.; and Xu, C. 2024. Adapt without forgetting: Distill proximity from dual teachers in vision-language models. In *European Conference on Computer Vision*, 109–125. Springer.
- Zheng, Z.; Ma, M.; Wang, K.; Qin, Z.; Yue, X.; and You, Y. 2023. Preventing zero-shot transfer degradation in continual learning of vision-language models. In *Proceedings of the IEEE/CVF international conference on computer vision*, 19125–19136.
- Zhu, H.; Wei, Y.; Liang, X.; Zhang, C.; and Zhao, Y. 2023. Ctp: Towards vision-language continual pretraining via compatible momentum contrast and topology preservation. In *Proceedings of the IEEE/CVF International Conference on Computer Vision*, 22257–22267.